NJC

Accepted Manuscript

This is an *Accepted Manuscript*, which has been through the Royal Society of Chemistry peer review process and has been accepted for publication.

Accepted Manuscripts are published online shortly after acceptance, before technical editing, formatting and proof reading. Using this free service, authors can make their results available to the community, in citable form, before we publish the edited article. We will replace this *Accepted Manuscript* with the edited and formatted *Advance Article* as soon as it is available.

You can find more information about *Accepted Manuscripts* in the Information for Authors.

Please note that technical editing may introduce minor changes to the text and/or graphics, which may alter content. The journal's standard Terms & Conditions and the Ethical guidelines still apply. In no event shall the Royal Society of Chemistry be held responsible for any errors or omissions in this *Accepted Manuscript* or any consequences arising from the use of any information it contains.

ROYAL SOCIETY OF CHEMISTRY

www.rsc.org/njc

A mononuclear gold(I) acetylide complex with amide group **3a** shows the dramatic color change towards F^- in DMSO.

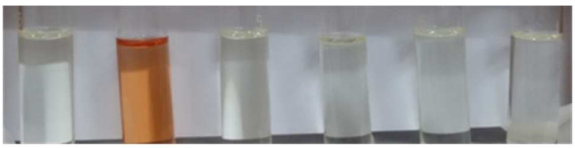

3a **3a**+F^- **3a**+Cl^- **3a**+OAc^- **3a**+Br^- **3a**+I^-

Journal Name

RSCPublishing

ARTICLE

Synthesis, Characterization, Photophysics, and Anion Binding Properties of Gold(I) Acetylide Complexes with Amide Group

Hua-Yun Shi, Jie Qi, Zhen-Ze Zhao, Wen-Juan Feng, Yu-Hao Li, Lu Sun, Zhuo-Jia Lin, Hsiu-Yi Chao*

Cite this: DOI: 10.1039/xoxxoooooox

Received ooth January 2012,
Accepted ooth January 2012

DOI: 10.1039/xoxxoooooox

www.rsc.org/

A series of mononuclear gold(I) acetylide complexes with amide group, $Ph_3PAuC{\equiv}CC_6H_4NHC(O)C_6H_4{-}R{-}4$ (R = NO_2 (**3a**), CF_3 (**3b**), H (**3c**), and OMe (**3d**)), have been synthesized and characterized. The crystal structure of $Ph_3PAuC{\equiv}CC_6H_4NHC(O)C_6H_4{-}NO_2{-}4$ (**3a**) was determined by X–ray diffraction. The photophysical properties of gold(I) acetylide complexes **3b**–**3d** have been studied. They show luminescence both in the solid state and in the degassed THF solution at 298 K. The anion-binding abilities of complexes **3a**–**3d** in $CDCl_3$ have also been studied by using ^1H NMR titration experiments. They show similar anion selectivity trend, and **3a** exhibits the highest binding affinity towards anions due to the strongest electron-withdrawing ability of NO_2 group among **3a**–**3d**. In DMSO, **3a** shows the dramatic color change towards F^- in DMSO, which provides an access of naked eye detection of F^-.

1. Introduction

Anions are one of the most important constituents of living systems because they play pivotal roles in ion transport, chemosensing and especially in the environment and in biology.[1–4] Since the first anion sensor reported by Park and Simmons in 1968,[5] anion sensors have attracted much attention and become an important field in supramolecular chemistry. Various methods have been applied to design an effective anion sensor over the past few decades. It usually consists of two main moieties: recognition unit and sensing unit. They are connected directly or by a spacer. When the recognition unit interacts with an anion by non-covalent interaction, the photophysical or redox properties of the sensing unit could be changed.[6–8] Thus, anion sensing can be realized by detecting receptors' optical and electrical signals. The observations in natural anion binding systems have motivated researchers to develop several artificial receptors employing hydrogen bonds offered by specific binding sites that are able to recognize and bind size- and shape-selective anionic guests on appropriate frameworks in various media.[9–10] To date, a number of synthetic receptors incorporating neutral N–H or cationic $(N–H)^+$ hydrogen bond donor, such as pyrrole,[11] ammonium,[12–13] guanidinium,[14] urea,[15–16] thiourea,[15] and amide,[17–19] have been proved to be particularly effective anion receptors in organic solvents. It is interesting to note that anion binding by proteins is most achieved by way of neutral amide functional groups employing the hydrogen bond donor of the N–H moiety.[20] Thus, amide-based organic anion sensors with aromatic or heterocyclic groups have been reported in the literature.[10,21] Their structures are simple and their modification can be easily carried out by organic synthesis.

Although most studies on the design of anion sensors in the past have been focused on organic receptors involving photo-induced electron transfer (PET) processes,[22] the utilization of transition metal complexes with amide group as anion sensors has been relatively less explored.[23–25] Compared to the common organic anion sensors, metal complexes with various properties like redox and luminescence were proved to be able to provide the various accesses of anion sensing. Some examples are ruthenium(II),[26–29] rhenium(I),[30–33] iridium(III),[34] platinum(II)[35–36] and gold(I)-copper(I)[37] complexes utilizing the MLCT or metal cluster-centered excited state for luminescent signal transduction. Among them, gold(I) complexes are one of the most important classes, for their intriguing photoluminescence behavior and their propensity to form aurophilic Au···Au interactions.[38] Many studies showed that the increase in the Au···Au interaction would lead to a shift of the emission to lower energy.[39] The preference of gold(I) for a linear coordination geometry, together with the linearity of the acetylide unit and its p-unsaturated nature, have made the gold(I) acetylide complexes attractive building blocks for organometallic oligomeric and polymeric materials, which may possess unique properties such as optical non-linearity, electrical conductivity, and liquid crystallinity.[40] The gold(I) acetylide complexes supported by an auxiliary phosphane ligand represents the major class of luminescent gold(I) complexes.[40] Che,[41–44] Yam,[45–50] and other groups[51–54] have studied the photophysical, photochemical, and ion-sensing properties of gold(I) acetylide complexes. However, to the best of our knowledge, no gold(I) acetylide complex with amide group has ever been reported as anion sensors until now.

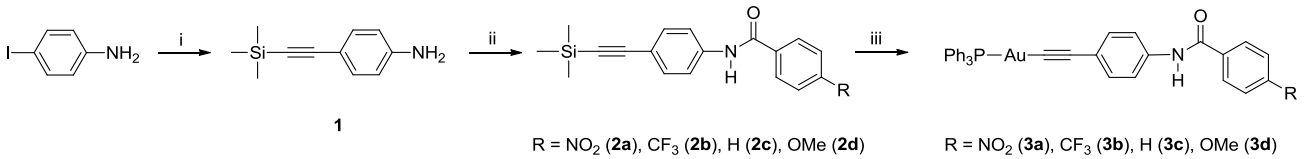

R = NO_2 (**2a**), CF_3 (**2b**), H (**2c**), OMe (**2d**) R = NO_2 (**3a**), CF_3 (**3b**), H (**3c**), OMe (**3d**)

Scheme 1. Synthetic route of gold(I) acetylide complexes **3a**–**3d**. i. $Pd(PPh_3)_2Cl_2$, CuI, $(CH_3)_3Si–C\equiv CH$, NEt_3, reflux, N_2, overnight; ii. $ClC(O)C_6H_4–R$, NEt_3, $CHCl_3$, reflux, N_2, overnight; iii. Ph_3PAuCl, $KF•2H_2O$, CH_2Cl_2/CH_3OH, dark.

Our group has a long-term interest in studying the relationship between the structures and properties of gold(I) acetylide complexes.[44, 53–54] We have synthesized a series of gold(I) acetylide complexes with urea or amide group, and studied their photophysical and ion-sensing properties.[53–54] To extend our study on gold(I) acetylide complexes with different anion binding ability, a series of mononuclear gold(I) acetylide complexes, $Ph_3PAuC\equiv CC_6H_4NHC(O)C_6H_4–R$–4 (R = NO_2 (**3a**), CF_3 (**3b**), H (**3c**), and OMe (**3d**); Scheme 1), have been synthesized and characterized in this work. The crystal structure of $Ph_3PAuC\equiv CC_6H_4NHC(O)C_6H_4–NO_2$–4 (**3a**) was determined by X–ray diffraction. We envisaged that if the photophysical properties of these gold (I) acetylide complexes could be changed when they interact with anions through hydrogen bonds between the amide N−H of the complexes and anions, they could be used as anion sensors. The only one binding site may match spherical anions better. The effect of the structure, especially the substituent R on the acetylide ligand of the complex, on the binding ability of the gold(I) acetylide complexes with anions has also been studied.

2. Results and discussion

2.1. Syntheses and Characterization

Scheme 1 shows the synthetic route of acetylide ligands with amide group (**2a**–**2d**) and mononuclear gold(I) acetylide complexes (**3a**–**3d**). The reaction of 4–[(trimethylsilyl)ethynyl]aniline with the corresponding acyl chloride in refluxing chloroform in the presence of triethylamine gave acetylide ligands **2a**–**2d**. Mononuclear gold(I) acetylide complexes **3a**–**3d** were obtained by the reaction of Ph_3PAuCl with the corresponding acetylide ligands **2a**–**2d** in a molar ratio of 1:1 in the presence of an excess of KF in dichloromethane/methanol mixture at 298 K. All gold (I) acetylide complexes **3a**–**3d** are air-stable in the solid state at 298 K and can be well dissolved in $CHCl_3$, CH_2Cl_2, THF and DMSO. They were all characterized by IR, ^1H NMR and ^{31}P NMR (Figure S1–S12, Supporting Information) and gave satisfactory elemental analysis.

The IR spectra of the gold(I) acetylide complexes **3a**–**3d** reveal the bands at 3389–3434 and 1656–1674 cm^{-1}, characteristic of the ν(N–H) and ν(C=O) of acetylide ligands, respectively. The ^1H NMR spectra of complexes **3a**–**3d** in $CDCl_3$ display a singlet at δ 7.68–7.84 ppm, which are assigned as the resonances of the amide N–H of the acetylide ligand. The chemical shifts of these peaks are in the following order: **3a** > **3b** ~ **3c** > **3d**, which is in line with the decreasing of the electron-withdrawing ability of substituent R on the acetylide ligand. In addition, the chemical shifts at δ 7.40–8.31 ppm are attributed to the resonances of the protons on the aromatic rings of the acetylide and triphehylphosphine ligands. The ^{31}P NMR spectra of the complexes **3a**–**3d** in $CDCl_3$ show a singlet at *ca.* δ 43.3 ppm. The NMR spectra of the complexes **3a**–**3d** are similar owing to their similar structure, and the substituent R on the acetylide ligand has a little effect on their chemical shifts.

2.2. Crystal Structure of 3a

The crystal structure of the mononuclear gold(I) acetylide complex **3a** has been determined by X–ray diffraction crystallography. The crystallographic data as well as selected bond distances and angles are listed in Table S1 (Supporting Information) and Table 1, respectively. Figure 1 shows the perspective drawing of **3a**. The triphenylphosphine ligand coordinates to the gold(I) metal center with the remaining site occupied by an acetylide ligand to give a nearly linear geometry. The C(1)–Au(1)–P(1), Au(1)–C(1)–C(2) and C(1)–C(2)–C(41) angles of 174.52(14) °, 174.3(5) ° and177.0(6) °, respectively, are deviated from the idealized values of 180 °, probably as a result of the steric demand of the ligands and crystal packing forces. The Au(1)–C(1) and Au(1)–P(1) bond distances for **3a** (2.012(5) and 2.2802(18)Å, respectively) are similar to those reported for other gold(I) arylacetylide complexes with triphenylphosphine ligand.[55–56] The C≡C bond distances (1.187(8) Å) are in the range typical of gold(I) acetylide systems.[44, 55–67] Because the angles of N(1)–C(3)–C(51), O(1)–C(3)–N(1) and O(1)–C(3)–C(51) are 115.7(5) °, 123.7(6) ° and 120.6(5) °, respectively, the geometry of the carbonyl group is nearly trigonal planar. The C=O distances for **3a** (1.217(7) Å) also resembles those in analogous gold(I) acetylide complexes with carbonyl group.[50] There are intermolecular hydrogen bond interactions between the hydrogen atom of amide group and the oxygen atom (O2) of nitro group in the acetylide ligands of **3a** (Figure 2). The hydrogen bond parameters of **3a** are listed in Table 2.

Table 1. Selected bond lengths (Å) and angles (°) for **3a**

Au(1)–C(1)	2.012(5)
Au(1)–P(1)	2.2802(18)
C(1)–C(2)	1.187(8)
C(3)–O(1)	1.217(7)
N(2)–O(2)	1.224(8)
N(2)–O(3)	1.215(7)
C(1)–Au(1)–P(1)	174.52(14)
Au(1)–C(1)–C(2)	174.3(5)
C(1)–C(2)–C(41)	177.0(6)
N(1)–C(3)–C(51)	115.7(5)
O(1)–C(3)–N(1)	123.7(6)
O(1)–C(3)–C(51)	120.6(5)
O(2)–N(2)–O(3)	124.0(6)

Table 2. Hydrogen bond parameters of **3a** (Å and °)

D–H ··A	d(D–H)	d(H ··A)	d(D ··A)	∠(DHA)
N(1)–H(1A) ··O(2)[a]	0.86	2.50	3.267(7)	149.7

[a]Symmetry transformations used to generate equivalent atoms: −x+4, y+4, z+2.

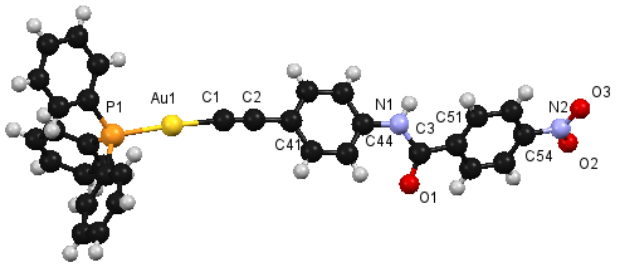

Fig. 1 Perspective view of **3a** with the atomic numbering scheme. Thermal ellipsoids are shown at the 30% probability level.

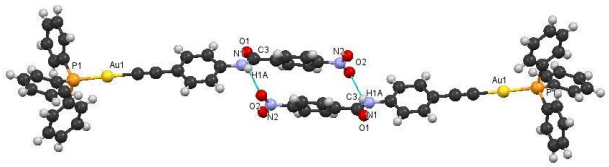

Fig. 2 Perspective view of two molecules of **3a** showing the intermolecular hydrogen bonding. Thermal ellipsoids are shown at the 30% probability level.

2.3. Electronic Absorption and Emission Spectra of Complexes 3a–3d

The photophysical data for complexes **3a**–**3d** are summarized in Table 3. Figure 3 shows the electronic absorption spectrum of **3a** in THF at 298 K. The absorption peak maxima of **3a** appear at 267, 277, 292, 305 and 330 nm. The spacings of adjacent absorption maxima of **3a** at 267–305 nm are *ca.* 1300–1800 cm^{-1}. Thus, the absorption bands of complex **3a** at 267–305 nm are assigned as the $\pi \rightarrow \pi^*$ transitions of the acetylide ligand.[54] The low-energy absorption band of **3a** at 330 nm could be due to the charge-transfer transition from the amide to the NO_2 group of the acetylide ligand.[54] The electronic absorption spectra of non-nitro derivatives **3b**–**3d** in THF at 298 K exhibit one shoulder (*ca*. 296 nm) and three bands (*ca*. 268, 277, and 312 nm) (Figures S13–S15, Supporting Information). The vibrational spacings are in three kinds of wavenumbers, *ca.* 1200, 1700 and 2200 cm^{-1}, which are ascribed to the phenyl ring deformation, C=O stretching, and C≡C stretching frequencies of the ground state, respectively.[44,54,58] These absorption bands are assigned to the $^1(\pi\pi^*)$ transition involving phenylic, carbonyl and acetylenic units of the acetylide ligand.

Upon excitation at λ > 300 nm, gold(I) acetylide complexes **3b**–**3d** in the solid state and THF solution exhibit luminescence in the visible light region at 298 K, with the emission quantum yields of 4.2×10^{-3}–1.02×10^{-2} in THF solution. Figures S16–S18 (Supporting Information) show the emission spectra of **3b**–**3d** in the solid state at room temperature. A broad band at *ca.* 471 nm is observed and its lifetime is in the microsecond range (Table 3). Thus, the emission is assigned to come from the $^3(\pi\pi^*)$ excited state of the acetylide ligand of gold(I) acetylide complexes. In THF, the emission spectra of complexes **3a**–**3d** exhibit three bands at *ca.* 408, 434 and 465 nm with the vibrational spacing of approximately 1300–1900 cm^{-1}, which are assigned to the stretching of phenyl and acetylene units of the acetylide ligand (Figures S19–S22, Supporting Information). Thus, the lowest-lying emissive state of complexes **3a**–**3d** in THF is assigned as the $^3(\pi\pi^*)$ excited state of the acetylide ligand, which is promoted through the spin−orbit coupling due to the introduction of gold atom.[54,58] For the mononuclear gold(I) acetylide complexes studied in this paper, except the nitro–derivatives **3a**, the substituent R on the acetylide ligand has little effect on the electronic absorption and emission spectra.

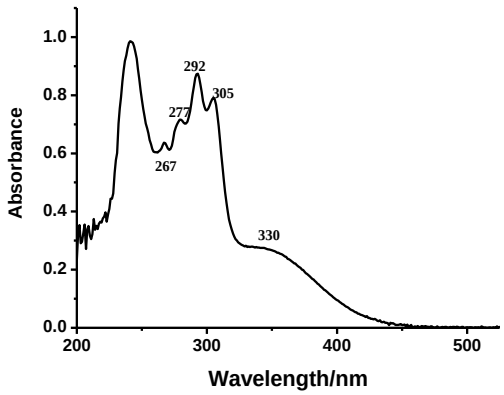

Fig. 3 The electronic absorption spectrum of **3a** (1.98×10^{-5} $mol\cdot dm^{-3}$) in THF at 298 K.

2.4. Anion Binding Properties of Complexes 3a–3d

Addition of the anions studied in this paper into the solutions of **3a**–**3d** did cause their UV-Vis spectral changes. However, these results could not be used to get accurate binding constants of complexes **3a**–**3d** towards anions. Thus, the interactions of **3a**–**3d** with anions in $CDCl_3$ have been investigated by ^1H NMR titration experiments. All of the anions used were in the form of tetra-*n*-butylammonium salts. Figure 4(a) shows the ^1H NMR spectral changes of **3a** upon addition of Cl^- in $CDCl_3$. The significant downfield shift of the signal of amide N–H (H_a) is observed upon addition of Cl^- from 0 to 5 equiv, while this peak has a little change upon addition of more than 5 equiv of Cl^-. Other protons' signals are found to undergo a little or relatively negligible changes, suggesting the formation of hydrogen bonds between the amide N–H of **3a** and Cl^-. The slight downfield shift of H_b and H_c on the phenyl ring is ascribed to the polarization effect of the C–H bond that is introduced by the through-space effect.[60–62] The ^1H NMR spectral changes of **3b**–**3d** upon gradual addition of Cl^- in $CDCl_3$ (Figures S31–32, S35–36, S43–44, Supporting Information) are similar to that of **3a**. Analogous investigations of **3a**–**3d** with Y–shape anion OAc^- or other halides such as F^-, Br^- and I^- in $CDCl_3$ have also been carried out. They show similar spectral changes in the ^1H NMR spectra (some are shown in Figures S23–S42, Supporting Information). The signals of amide N–H (H_a) exhibit a significant downfield shift of 0.6 to 2.8 ppm, while the signals of aromatic proton shift relatively less. The extent of the shift of H_a upon the addition of Br^-, I^-, and OAc^- is found to be obviously smaller than that of Cl^-, while the addition of F^- induced the disappearance of the amide N–H signals for **3a** and **3b**, but a larger shift for **3c** and **3d**. Figure S45 (Supporting Information) shows the shifts of the signals of amide N–H (H_a) of **3c** upon addition of different anions in $CDCl_3$ at 298 K. Unfortunately, the binding constant of **3c** with F^- can only be determined because the signals of amide N–H (H_a) of **3d** is too broad to be detected after the addition of 5 equiv of F^-.

To determine the binding ratio between gold(I) acetylide complexes **3a**–**3d** and anions, Job's plot analysis has been carried out. Figure 5 shows the Job's plots of **3b** with Cl^-, Br^-, I^-, and OAc^- in $CDCl_3$. A plot of the changes of chemical shift of N–H versus X_{3b} (= [**3b**] / ([Anion] + [**3b**])) shows a break point at a molar ratio of *ca*. 0.5, indicative of a 1:1 complexation stoichiometry.

Table 3. Photophysical data of complexes **3a**–**3d** at 298 K.

complex	medium	λ_{abs} / nm (ε / $dm^3mol^{-1}cm^{-1}$)	λ_{em} / nm (τ_{em} / μs)	Φ^a
3a	THF	267 (32170), 277 (35350), 292 (sh, 44040), 305 (39950), 330 (14240)	408 (max), 434, 465	0.0042
	solid		non-emissive	
3b	THF	268 (17420), 276 (20000), 296 (sh, 25810), 315 (34950)	408 (max), 432, 465	0.0059
	solid		471 (2.6)	
3c	THF	267 (16310), 276 (18640), 296 (sh, 33230), 314 (43640)	407 (max), 434, 465	0.0050
	solid		471 (2.5)	
3d	THF	268 (19900), 277 (22420), 296 (sh, 37630), 312 (47320)	410 (max), 432, 471	0.0102
	solid		484 (3.5)	

[a] Quinine sulfate as reference.[59]

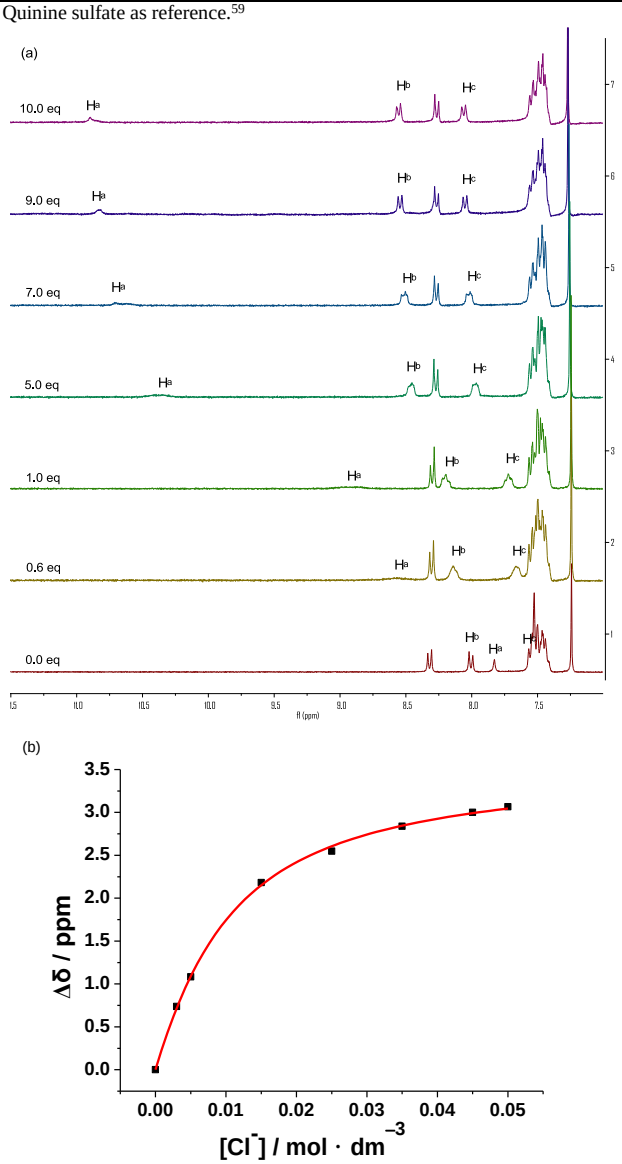

Fig. 4 (a) ^{1}H NMR spectral changes of **3a** upon addition of Cl^-. (b) The corresponding binding plot (the shifts of the signals of amide proton H_a as a function of [Cl^-] and its theoretical fit for the 1:1 binding of **3a** with Cl^-).

Using the 1:1 binding model, the anion-binding constants of complexes **3a**–**3d** were obtained by nonlinear least-square fits of the shifts of the signals of amide N–H (H_a) versus the concentration of the added anions. The binding constants (*K*) for different anions are summarized in Table 4. In general, the binding constants of different complexes with the same anion are in the following order: R = NO_2 (**3a**) > CF_3 (**3b**) > H (**3c**) ≈ OCH_3 (**3d**), which is in line with the decreasing of the electron-withdrawing ability of substituent R on the acetylide ligands. This could be rationalized by the fact that the interactions between complexes (**3a**–**3d**) and anions are hydrogen bonds in nature and the stronger hydrogen bond acceptor, which could be induced by the stronger electron-withdrawing group, could form stronger hydrogen bonds. The *K* values of the same complex with the various anions are in the following order: Cl^- > OAc^- ≈ Br^- > I^- (F^- > Cl^- > OAc^- ≈ Br^- > I^- for **3c**), which is almost in line with the decreasing of the basicity of anions (F^- > OAc^- >Cl^- > Br^- > I^-). The Cl^- > OAc^- order could be due to the mismatching between the mono hydrogen bond donor N–H and Y-shape OAc^- (two hydrogen bond donor).

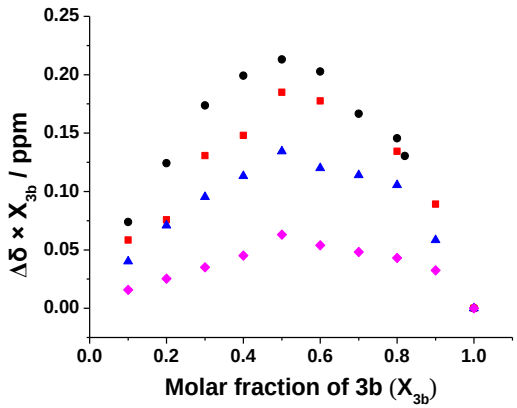

Fig. 5 Job's plots of complex **3b** with Cl^- (●), Br^- (▲), I^- (◆), and OAc^- (■) in $CDCl_3$ ([**3b**] + [anion] = 5.0×10^{-3} mol·dm^{-3})

To confirm the reliability of our results about the order of the affinity between gold(I) acetylide complexes **3a**–**3d** and anions, the anion-binding constants of the acetylide ligands, HC≡$CC_6H_4NHC(O)C_6H_4$–R–4 (R = NO_2 (**4a**), CF_3 (**4b**), H (**4c**), and OMe (**4d**)), have also been determined (Figures S46−S63 and Table S2, Supporting Information). For the same anion, the binding constants of the acetylide ligands are in the following order: R = NO_2 (**4a**) > CF_3 (**4b**) > H (**4c**) ≈ OCH_3 (**4d**). For the same ligand, the *K* values with various anions are in the following order: Cl^- > OAc^- ≈ Br^- > I^-. These orders are in line with those observed in complexes **3a**–**3d**. In general, the acetylide ligands **4a**–**4d** have larger anion-binding constants than their corresponding gold(I) acetylide complexes **3a**–**3d** in $CDCl_3$.

The interaction of **3a** with F^- was investigated in different solvents. Figure S23 (Supporting Information) shows the ^{1}H NMR spectral changes of **3a** in $CDCl_3$ upon addition of F^-, which are quite different from those of **3a** with Cl^- in $CDCl_3$ (Figure 4(a)). When 0.2 equiv of F^- was added to the $CDCl_3$ solution of **3a**, the signals of the

N–H proton disappeared rapidly, and the aromatic proton signals H_b and H_c showed a slight downfield shift. During the addition of F^-, the color of the solution of **3a** in $CDCl_3$ changes from light yellow to bright yellow (Figure 6). On the other hand, when 10 equiv of F^- was added into the **3a** solution in DMSO-d_6, the solution shows dramatic color change from light yellow to dark red (Figure 6). Figure S64(a) (Supporting Information) show the ^1H NMR spectrum of **3a** in DMSO–d_6 upon addition of 10 equiv of F^-. The signals of the N–H proton disappear again and a distinct triplet centered at 16.08 ppm (J = 120 Hz) appears, which is assigned as the formation of HF_2^-.[63–64] In addition, its ^{19}F NMR spectrum also display a distinct doublet centered at –143.13 ppm (J = 117 Hz) (Figure S65, Supporting Information), suggesting the formation of HF_2^-.[63–64] These results indicate the deprotonation of the amide N–H of **3a** upon addition of F^- in DMSO–d_6.

We have also examined the color change of complexes **3a** with different anions in DMSO. Except **3a** with F^- in DMSO, no significant color change could be observed (Figures S66 and S67, Supporting Information). Thus, **3a** shows the selective color change towards F^- in DMSO. Considering the different colour change upon the addition of various anions, the anion-sensing properties of complexes **3b**–**3d** with different anions have also been examined in different solvents. However, no significant color changes were observed.

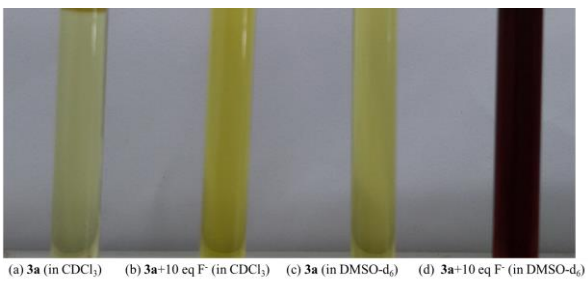

Fig. 6 Colors of the solutions: (a) **3a** in $CDCl_3$. (b) **3a** + 10 eq F^- in $CDCl_3$. (c) **3a** in DMSO-d_6. (d) **3a** + 10 eq F^- in DMSO-d_6. The concentration of **3a** is 5.0×10^{-3} mol dm^{-3}.

3. Conclusions

In this work, amide based gold(I) acetylide complexes **3a**–**3d** have been synthesized and characterized. Complexes **3b**–**3d** show luminescence both in the solid state and in the degassed THF solution at 298 K. In $CDCl_3$, the binding constants of **3a**–**3d** with the same anion are in the following order: R = NO_2 (**3a**) > CF_3 (**3b**) > H (**3c**) ≈ OCH_3 (**3d**). For the same complex, the order follows Cl^- > OAc^- ≈ Br^- > I^-. In DMSO, **3a** shows the selective color change towards F^-. This makes the naked eye detection of F^- become possible. We envisage this class of gold(I) complexes could have potential applications in life science and environmental science by using the water-soluble auxiliary ligands.

4. Experimental

4.1. Materials and reagents

Ph_3PAuCl[65] and 4–[(trimethylsilyl)ethynyl]aniline[66] were synthesized according to literature procedures. 4–Nitrobenzoyl chloride was purchased from TCI. 4–Iodoaniline, benzoyl chloride, tetra-*n*-butylammonium chloride hydrate were obtained from Alfa–Aesar. 4–Methoxybenzoyl and 4–trifluoromethylbenzoyl chloride were purchased from J&K. Tetra-*n*-butylammonium fluoride hydrate and tetra-*n*-butylammonium acetate were obtained from Sigma–Aldrich. All reactions were carried out under anhydrous and anaerobic conditions using standard Schlenk techniques under nitrogen. All solvents were purified and distilled using standard procedures before use. All other reagents were of analytical grade and were used as received.

4.2. Physical measurements and instrumentation

Chemical shifts (δ, ppm) were reported relative to tetramethylsilane for ^1H NMR, 85% H_3PO_4 for ^{31}P NMR, and NaF (δ = –122.4) for ^{19}F NMR on a Varian Mercury–Plus 300 spectrometer. Electronic absorption spectra were measured on a PGENERAL TU1901 UV–vis spectrophotometer. Emission spectra were obtained on a FLSP920 fluorescence spectrophotometer. Solution samples for emission spectra were degassed by four freeze–pump–thaw cycles.

4.3. Crystal structure determination

Crystals of **3a** were grown by diffusion of diethyl ether into THF solution of **3a**. Selected single crystals of **3a** were used for data collection on a Bruker SMART 1000 CCD diffractometer with graphite monochromatized Mo–Kα radiation (λ = 0.710×73 Å) at 110 K. An empirical absorption correction was applied using the SADABS program. The structures were solved by direct methods and refined by full-matrix least-squares based on F^2 using the SHELXTL program package.[67] CCDC 1013703 contain the supplementary crystallographic data for **3a**. These data can be obtained free of charge via http://www.ccdc.cam.ac.uk/conts/retrieving.html, or from the Cambridge Crystallographic Data Center, 12 Union Road, Cambridge CB2 1EZ, U.K.; fax:(+44) 1223 336-033; or e-mail deposit@ccdc.cam.ac.uk

4.4. Titrations and Job's plot

For a typical ^1H NMR titration experiment, 1 μL aliquots of a tetra-*n*-butylammonium salt (1.00×10^{-3} mol·dm^{-3} in $CDCl_3$) were added into the 0.5 mL solution of the gold(I) acetylide complex in $CDCl_3$ (5.00×10^{-3} mol·dm^{-3}) by a syringe, and the ^1H NMR spectral changes were recorded by a Varian Mercury–Plus 300 spectrometer at 298 K. The binding constant K values were determined by nonlinear fitting using 1:1 model. Job's plots were obtained from a series of solutions in which the fraction of the corresponding anions varied, keeping the total concentration (the complexes and anions) constant. The maxima of the plots indicated the binding stoichiometry of the complexes with anions.

4.5. Synthesis

4.5.1. Sythesis of acetylide ligands **2a**–**2d**

$(CH_3)_3SiC{\equiv}CC_6H_4NHC(O)C_6H_4$–$NO_2$ –4 (**2a**)

To a solution of 4–[(trimethylsilyl)ethynyl]aniline (100.8 mg, 0.53 mmol) and 4–nitromethylbenzoyl chloride (99.8 mg, 0.54 mmol) in $CHCl_3$ was added triethylamine (0.8 ml). The mixture was heated to reflux for 18 h. The solvent was removed under reduced pressure, and the residue was washed with water and *n*-hexane to yield a pale yellow solid. Yield: 116.3 mg, 65 %. ^1H NMR (300 MHz, $CDCl_3$, 298K): δ = 8.31 (d, 2H, J = 9 Hz, aromatic ring), 8.00 (d, 2H, J = 9 Hz, aromatic ring), 7.97 (s, 1H, NH), 7.59 (d, 2H, J = 9 Hz, aromatic ring), 7.47 (d, 2H, J = 9 Hz, aromatic ring), 0.26 (s, 9H, CH_3). IR (KBr, cm^{-1}): ν = 3318 (N–H), 2154 (C≡C), 1660 (C=O). Anal.

Table 4. Binding constants of **3a**–**3d** for anions in $CDCl_3$.[a]

complex	F^-	Cl^-	OAc^-	Br^-	I^-
3a	[b]	126.40 ±6.13	77.35 ±7. 80	86.71 ±3.76	40.96 ±2.56
3b	[b]	61.00 ±5.54	47.28 ±2.38	41.46 ±1.84	30.53 ±3.73
3c	24.87 ±3.57	15.02 ±1.42	7.18 ±1.11	6.87 ±0.83	4.85 ±0.84
3d	[b]	15.56 ±1.65	8.02 ±1.28	8.95 ±1.29	[b]

[a] Binding constants were determined by 1:1 model using the nonlinear fitting method. [b]Chemical shifts were not suitable for accurate measurement of binding constants.

Calcd for $C_{18}H_{18}N_2O_3Si$ (%): C, 63.88; H, 5.36; N, 8.28. Found: C, 64.03; H, 5.37; N, 8.31.

$(CH_3)_3SiC{\equiv}CC_6H_4NHC(O)C_6H_4{-}CF_3{-}4$ (**2b**)

To a solution of 4–[(trimethylsilyl)ethynyl]aniline (134.7 mg, 0.65 mmol) and 4–trifluorobenzoyl chloride (121.6 mg, 0.64 mmol) in $CHCl_3$ was added triethylamine (0.8 ml). The mixture was heated to reflux for 18 h. The solvent was removed under reduced pressure, and the residue was washed with water and *n*-hexane to yield a pale incarnadine solid. Yield: 132.3 mg, 57 %.^{1}H NMR (300 MHz, $CDCl_3$, 298K): δ = 7.94 (d, 2H, J = 8 Hz, aromatic ring), 7.85 (s, 1H, NH), 7.73 (d, 2H, J = 8 Hz, aromatic ring), 7.59 (d, 2H, J = 8 Hz, aromatic ring), 7.46 (d, 2H, J = 9 Hz, aromatic ring), 0.26 (s, 9H, CH_3). IR (KBr, cm^{-1}): ν = 3432 (N−H), 2162 (C≡C), 1657 (C=O). Anal. Calcd for $C_{19}H_{18}F_3NOSi$ (%): C, 63.14; H, 5.02; N, 3.88. Found: C, 63.40; H, 5.03; N, 3.90.

$(CH_3)_3SiC{\equiv}CC_6H_4NHC(O)C_6H_5$ (**2c**)

To a solution of 4–[(trimethylsilyl)ethynyl]aniline (101.4 mg, 0.54 mmol) and benzoyl chloride (76.6 mg, 0.54 mmol) in $CHCl_3$ was added triethylamine (0.8 ml). The mixture was heated to reflux for 18 h. The solvent was removed under reduced pressure, and the residue was washed with water and *n*-hexane to yield a yellow solid. Yield: 95.5 mg, 61 %.^{1}H NMR (300 MHz, $CDCl_3$, 298K): δ = 7.85–7.82 (m, 3H, NH + aromatic ring), 7.59 (d, 2H, J = 9 Hz, aromatic ring), 7.54–7.44 (m, 5H, aromatic ring), 0.25 (s, 9H, CH_3). IR (KBr, cm^{-1}): ν = 3270 (N–H), 2156 (C≡C), 1647 (C=O). Anal. Calcd for $C_{18}H_{19}NOSi$ (%): C, 73.68; H, 6.53; N, 4.77. Found: C, 73.38; H, 6.54; N, 4.78.

$(CH_3)_3SiC{\equiv}CC_6H_4NHC(O)C_6H_4{-}OMe{-}4$ (**2d**)

To a solution of 4–[(trimethylsilyl)ethynyl]aniline (104.9 mg, 0.55 mmol) and 4–methoxybenzoyl (94.4 mg, 0.55 mmol) in $CHCl_3$ was added triethylamine (0.8 ml). The mixture was heated to reflux for 18 h. The solvent was removed under reduced pressure, and the residue was washed with water and *n*-hexane to yield a pale yellow solid. Yield: 119.4 mg, 67 %.^{1}H NMR (300 MHz, $CDCl_3$, 298K): δ = 7.81–7.77 (m, 3H, NH + aromatic ring), 7.57 (d, 2H, J = 8 Hz, aromatic ring), 7.43 (d, 2H, J = 8 Hz, aromatic ring), 6.93 (d, 2H, J = 9 Hz, aromatic ring), 3.85 (s, 3H, OCH_3), 0.25 (s, 9H, CH_3). IR (KBr, cm^{-1}): ν = 3436 (N−H), 2152 (C≡C), 1649 (C=O). Anal. Calcd for $C_{19}H_{21}NO_2Si$ (%): C, 70.55; H, 6.54; N, 4.33. Found: C, 70.61; H, 6.55; N, 4.34

4.5.2. Sythesis of gold(I) acetylide complexes **3a**–**3d**

$Ph_3PAuC{\equiv}CC_6H_4NHC(O)C_6H_4{-}NO_2{-}4$ (**3a**)

To a mixture of Ph_3PAuCl (51.0 mg, 0.1031 mmol) and **2a** (34.9 mg, 0.1031 mmol) in CH_2Cl_2 was added KF $2H_2O$ (19.2 mg, 0.2040 mmol) in methanol dropwise. The mixture was stirred overnight in the dark. After evaporation to dryness, the solid residue was extracted with THF. Subsequent diffusion of diethyl ether into the concentrated THF solution gave light yellow crystals. Yield: 53.8 mg, 72 %.^{1}H NMR (300 MHz, $CDCl_3$, 298K): δ = 8.31 (d, 2H, J = 9 Hz, aromatic ring), 8.00 (d, 2H, J = 9 Hz, aromatic ring), 7.84 (s, 1H, NH), 7.56–7.40 (m, 19H, aromatic ring). ^{31}P NMR ($CDCl_3$, 298K): δ = 43.27. IR (KBr, cm^{-1}): ν = 3389 (N–H), 1674 (C=O). Anal. Calcd for $C_{33}H_{24}AuN_2O_3P$ (%): C, 54.71; H, 3.34; N, 3.87. Found: C, 54.55; H, 3.88; N, 3.87.

$Ph_3PAuC{\equiv}CC_6H_4NHC(O)C_6H_4{-}CF_3{-}4$ (**3b**)

To a mixture of Ph_3PAuCl (51.3 mg, 0.1037 mmol) and **2b** (37.6 mg, 0.1040 mmol) in CH_2Cl_2 was added KF $2H_2O$ (19.5 mg, 0.2072 mmol) in methanol dropwise. The mixture was stirred overnight in the dark. After evaporation to dryness, the solid residue was extracted with CH_2Cl_2. Subsequent diffusion of diethyl ether into the concentrated CH_2Cl_2 solution gave pale yellow crystals. Yield: 40.1 mg, 52 %.^{1}H NMR (300 MHz, CDCl3, 298K): δ = 7.95 (d, 2H, J = 8 Hz, aromatic ring), 7.77 (s, 1H, NH), 7.73 (d, 2H, J = 8 Hz, aromatic ring), 7.57–7.40 (m, 19H, aromatic ring). ^{31}P NMR ($CDCl_3$, 298K): δ = 43.31. IR (KBr, cm^{-1}): ν = 3432 (N–H), 1666 (C=O). Anal. Calcd for $C_{34}H_{24}AuF_3NOP$ (%): C, 54.63; H, 3.24; N, 1.87. Found: C, 54.50; H, 3.24; N, 1.86.

$Ph_3PAuC{\equiv}CC_6H_4NHC(O)C_6H_5$ (**3c**)

To a mixture of Ph_3PAuCl (55.6 mg, 0.1124 mmol) and **2c** (34.5 mg, 0.1175 mmol) in CH_2Cl_2 was added KF $2H_2O$ (24.8 mg, 0.2645 mmol) in methanol dropwise. The mixture was stirred overnight in the dark. After evaporation to dryness, the solid residue was extracted with THF. Subsequent diffusion of diethyl ether into the concentrated THF solution gave yellow crystals. Yield: 51.4 mg, 67 %.^{1}H NMR (300 MHz, $CDCl_3$, 298K): δ = 7.83 (d, 2H, J = 7 Hz, aromatic ring), 7.77 (s, 1H, NH), 7.57–7.40 (m, 22H, aromatic ring). ^{31}P NMR ($CDCl_3$, 298K): δ = 43.32. IR (KBr, cm^{-1}): ν = 3434 (N−H), 1657 (C=O). Anal. Calcd for $C_{33}H_{25}AuNOP$ (%): C, 58.33; H, 3.71; N, 2.06. Found: C, 58.35; H, 3.72; N, 2.07.

$Ph_3PAuC{\equiv}CC_6H_4NHC(O)C_6H_4{-}OMe{-}4$ (**3d**)

To a mixture of Ph_3PAuCl (51.8 mg, 0.1047 mmol) and **2d** (34.5 mg, 0.1067 mmol) in CH_2Cl_2 was added KF $2H_2O$ (24.9 mg, 0.2645 mmol) in methanol dropwise. The mixture was stirred overnight in the dark. After evaporation to dryness, the solid residue was extracted with CH_2Cl_2. Subsequent diffusion of diethyl ether into the concentrated CH_2Cl_2 solution gave pale yellow crystals. Yield: 44.3 mg, 60 %.^{1}H NMR (300 MHz, $CDCl_3$, 298K): δ = 7.80 (d, 2H, J = 9 Hz, aromatic ring), 7.68 (s, 1H, NH), 7.57–7.40 (m, 19H, aromatic ring), 6.95 (d, 2H, J = 9 Hz, aromatic ring), 3.85 (s, 3H, CH_3). ^{31}P NMR ($CDCl_3$, 298K): δ = 43.34. IR (KBr, cm^{-1}): ν = 3430 (N–H), 1662 (C=O). Anal. Calcd for $C_{34}H_{27}AuNO_2P$ (%): C, 57.55; H, 3.84; N, 1.97. Found: C, 57.61; H, 3.85; N, 1.96.

Acknowledgements

We acknowledge financial support from the National Natural Science Foundation of China (20971131, J1103305), the Natural Science Foundation of Guangdong Province (S2012010010566), the Undergraduate Innovative Experiment Program of Guangdong Province (1055812184), and Sun Yat-Sen University. We thank Dr. Xiao-Long Feng for crystallographic data collection. We also thank the editors and reviewers for helpful comments and suggestions.

Notes and references

MOE Key Laboratory of Bioinorganic and Synthetic Chemistry, School of Chemistry and Chemical Engineering, Sun Yat-Sen University, Guangzhou 510275, P. R. China. E-mail: zhaoxy@mai l.sysu.edu.cn; Fax: +86-20-84112245; Tel: +86-20-84110062.

Electronic Supplementary Information (ESI) available: A X-ray crystallographic file in CIF format for complex **3a**. Additional figures and tables.. See DOI: 10.1039/b000000x/

1. Z. Xu, X. Chen, H. N. Kim, J. Yoon, *Chem. Soc. Rev.* , 2010 , **39** , 127.
2. S. Kubik, *Chem. Soc. Rev.*, 2010, *39*, 3648.
3. B. Valeur, I. Leray, *Coord. Chem. Rev.*, 2000, **205**, 3.
4. C. Caltagirone, P. A. Gale, *Chem. Soc. Rev.*, 2009, **38**, 520.
5. C. H. Park, H. E. Simmons, *J. Am. Chem. Soc.*, 1968 , **90**, 2431.
6. J. W. Steed, *Chem. Soc. Rev.*, 2009, **38**, 506.
7. V. Balzani, N. Sabbatina, F. Scandola, *Chem. Rev.*, 1986, **86**, 319.
8. D. B. MacQueen, K. S. Schanze, *J. Am. Chem. Soc.*, 1991, **113**, 6108.
9. M. Arunachalam, P. Ghosh, *Inorg. Chem.*, 2010, **49**, 943.
10. C. R. Bondy, S. J. Loeb, *Coord. Chem. Rev.*, 2003, **240**, 77.
11. M. P. Wintergerst, T. G.Levitskaia, B. A.Moyer, J. L.Sessler, L. H. Delmau, *J. Am. Chem. Soc.*, 2008, **130**, 4129.
12. J. Fitzmaurice, G. M. Kyne, D. Douheret, J. D. Kilburn, *J. Chem. Soc., Perkin Trans*. 2002, **1**, 841.
13. J. Yoon, S. K. Kim, N. J. Singh, K. S. Kim, *Chem. Soc. Rev.*, 2006, **35**, 355.
14. M. D. Best, S. L. Tobey, E. V. Anslyn, *Coord. Chem. Rev.*, 2003, **240**, 3.
15. A. F. Li, J. H. Wang, F. Wang, Y. B. Jiang, *Chem. Soc. Rev.*, 2010, **39**, 3729.
16. L. Fabbrizzi, V. Amendola, L. Mosca, *Chem. Soc. Rev.*, 2010, **39**, 3889.
17. G.Kumaresh, A. R. Sarkar, A. Ghorai, U. Ghosh, *New J. Chem.*, 2012, **36**, 1231.
18. P. A. Gale, K. Navakhun, S. Camiolo, M. E. Light, M. B. Hursthouse, *J. Am. Chem. Soc.*, 2002, **124**, 11228.
19. S. Camiolo, P. A. Gale, M. B. Hursthouse, M. E. Light, A. J. Shi, *Chem. Commun.*, 2002, 758.
20. D. Voet, J.G. Voet, C.W. Pratt. Fundamentals of Biochemistry, Wiley, New York, 1999.
21. P. Dydio, D. Lichosyt, J. Jurczak, *Chem. Soc. Rev.*, 2011, **40**, 2971.
22. A. W. Czarnik. Fluorescent Chemosensors for Ion and Molecule Recognition, ACS, Washington, 1993.
23. L. J. Kuo, J. H. Liao, C. T. Chen, C. H. Huang, C. S. Chen, J. M. Fang, *Org. Lett.*, 2003, **5**, 1821.
24. S. Shanmugaraju, A. K. Bar, K. W. Chi, P. S. Mukherjee, *Organometallics.*, 2010, **29**, 2971.
25. S. S. Sun, A. J. Lees, P. Y. Zavalij, *Inorg. Chem.*, 2003, **42**, 3445.
26. Y. Cui, H. J. Mo, J. C. Chen, Y. L. Niu, Y. R. Zhong, K. C. Zheng, B. H. Ye, *Inorg. Chem.*, 2007, **46**, 6427.
27. Y. Cui, Y. L. Niu, M. L. Cao, K. Wang, H. J. Mo, Y. R. Zhong, B. H. Ye, *Inorg. Chem.*, 2008, **47**, 5616.
28. T. P. Lin, C. Y. Chen, Y. S. Wen, S. S. Sun, *Inorg. Chem.*, 2007, **42**, 9201.
29. J. L. Fillaut, J. Andries, L. Toupet, J. P. Desvergne, *Chem. Commun.*, 2005, **23** 2524.
30. C. Y. Hung, A. S. Singh, C. W. Chen, Y. S. Wen, S. S. Sun, A. J. Lees, *Chem. Commun.*, 2009, **12** 1511.
31. C. Y. Hung, A. S. Singh, C. W. Chen, Y. S. Wen, S. S. Sun, *Chem. Commun*. 2009, **12**, 1511.
32. A. Bessette, S. Nag, A. K. Pal, S. Derossi, G. S. Hanan, *Supramol. Chem*. 2012, **24**, 595.
33. T. Lazarides, T. A. Miller, J. C. Jeffer, T. K. Ronson, H. Adams, M. D. Ward, *Dalton Trans.*, 2005, 528.
34. (a) Q. Zhao, T. Cao, F. Li, X. Li, H. Jing, T. Yi, C. Huang, *Organometallics*, 2007, **26**, 2077. (b) X. Yang, Z. Huang, C. L. Ho, G. Zhou, D. R. Whang, C. Yao, X. Xu, S. Y. Park, C. H. Chui, W. Y. Wong, *RSC Adv.*, 2013,**3**, 6553.
35. (a) J. L. Fillaut, H. Akdas-Kilig, E. Dean, C. Latouche, A. Boucekkine, *Inorg. Chem.*, 2013, **52**, 4890. (b) X. Yang, Z. Huang, J. Dang, C. L. Ho, G. Zhou,W. Y. Wong, *Chem. Commun.*, 2013,**49**, 4406.
36. (a) C. Qin, W. Y. Wong, L. Wang, *Macromolecules*, 2011, **44**, 483. (b) Y. Fan, Y. M. Zhu, F. R. Dai, L. Y. Zhang, Z. N. Chen, *Dalton Trans.*, 2007, **35**, 3885.
37. X. He, N. Zhu, V. W. W. Yam, *Dalton Trans.*, 2011, **40**, 9703.
38. (a) P. Pyykkö, *Angew. Chem., Int. Ed.*, 2004, **43**, 4412. (b) P. Li, B Ahrens, K. H. Choi, M. S. Khan, P. R. Raithby, P. J. Wilson, W. Y. Wong, *CrystEngComm*, 2002,**4**, 405.
39. V. W. W. Yam, E. C. C. Cheng, *Chem. Soc. Rev.*, 2008, **37**, 1806.
40. (a) J. C. Lima, L. Rodriguez, *Chem. Soc. Rev*., 2011, **40**, 5442. (b) W. Y. Wong, *Coord. Chem. Rev*., 2007, **251**, 2400. (c) S. Y. Poon1, W. Y. Wong, K. W. C., J. X. Shi, *Chem. Eur. J*., 2006, **12**, 2550. (d) W. Y. Wong, *Comment Inorg. Chem.*, 2005, **26**, 39. (e) W. Y. Wong, K. H. Choi, G. L. Lu, J. X. Shi, P. Y. Lai, S. M. Chan, Z. Lin, *Organometallics*, 2001, **20**, 5446.
41. D. Li, X. Hong, C. M. Che, W. C. Lo, S. M. Peng, *Dalton Trans*., 1993, **19**, 2929.
42. W. Lu, W. M. Kwok, C. Ma, C. T. L. Chan, M. X. Zhu, C. M. Che, *J. Am. Chem. Soc.*, 2011, **133**, 14120.
43. A. L. F. Chow, M. H. So, W. Lu, N. Y. Zhu, C. M. Che, *Chem. Asian J*., 2011, **6**, 544.
44. H. Y. Chao, W. Lu, Y. Li, M. C. W. Chan, C. M. Che, K. K. Cheung, N. Zhu, *J. Am. Chem. Soc.*, 2002, **124**, 14696.
45. X. X. Lu, C. K. Li, E. C. C. Cheng, N. Zhu, V. W. W. Yam, *Inorg. Chem.*, 2004, **43**, 2225.
46. X. He, W. Lam, N. Zhu, V. W. W. Yam, *Chem. Eur. J*., 2009, **15**, 8842.
47. S. K. Yip, E. C. C. Cheng, L. H. Yuan, N. Zhu, V. W. W. Yam, *Angew. Chem., Int. Ed.*, 2004, **43**, 4954.
48. V. W. W. Yam, C. K. Li, C. L. Chan, *Angew. Chem., Int. Ed.*, 1998, **37**, 2857.
49. X. He, E. C. C. Cheng, N. Zhu, V. W. W. Yam, *Chem. Commun.*, 2009, **27**, 4016.
50. H. S. Tang, N. Y. Zhu, V. W. W. Yam, *Organometallics.*, 2007, **26**, 22.
51. I. O. Koshevoy, C. Li. Lin, C. C. Hsieh, A. J. Karttunen, M. Haukka, T. A. Pakkanen, P. T. Chou, *Dalton Trans.*, 2012, **41**, 937.
52. Q. Y. Hu, W. X. Lu, H. D. Tang, H. H. Y. Sung, T. B. Wen, I. D. Williams, G. K. L. Wong, Z. Lin, G. Jia, *Organometallics.*, 2005, **24**, 3966.
53. Y. P. Zhou, E. B. Liu, J. Wang, H. Y. Chao, *Inorg. Chem.*, 2013, **52**, 8629.
54. Y. P. Zhou, M. Zhang, Y. H. Li, Q. R. Guan, F. Wang, Z. J. Lin, C. K. Lam, X. L. Feng, H. Y. Chao, *Inorg. Chem.*, 2012, **51**, 5099.
55. D. Castillo, J. Trevor, S. Sarkar, K. A. Abboud, A. S. Veige, *Dalton Trans*., 2011, **40**, 8140.
56. M. C. Blanco, J. Camara, M. C. Gimeno, P. G. Jones, A. Laguna, J. M.

Lopez-de-Luzuriaga, M. E. Olmos, M. D. Villacampa, *Organometallics*., 2011, **31**, 2597.
57. D. E. Gomez, L. Fabbrizzi, M. Licchelli, E. Monzani, *Org. Biomol. Chem.*, 2005, **3**, 1495.
58. C. M. Che, H. Y. Chao, V. M. Miskowski, Y. Li, K. K. Cheung, *J. Am. Chem. Soc*., 2001, **123**, 4985.
59. J. N. Demasa, G. A. Crosby, *J. Phy. Chem.*, 1971, 75, 991.
60. D. Esteban-Gomez, L. Fabbrizzi, M. Liechelli, *J. Org. Chem.*, 2005, **70**, 5717.
61. M. Boiocchi, L. DelBoca, D. Esteban-Gomez, L. Fabbrizzi, M. Licchelli, E. Monzani, *Chem. Eur. J.*, 2005, **11**, 3097.
62. M. Boiocchi, L. DelBoca, D. E. Gomez, L. Fabbrizzi, M. Licchelli, E. Monzani, *J. Am. Chem. Soc.*, 2004, **126**, 16507.
63. A. B. Descalzo, K. Rurack, H. Weisshoff, R. Martínez-Máñez, M. D. Marcos, P. Amorós, K. Hoffmann, J. Soto, *J. Am. Chem. Soc.*, 2004, **127**, 184.
64. C. Jia, B. Wu, J. Liang, X. Huang, X. Yang, *J. Fluoresc.*, 2010, **20**, 291.
65. A. K. Al-sa'ady, C. A. McAuliffe, R. V. Parish, J. A. Sandbank, *Inorg. Synth.*, 1985, **23**, 191.
66. P. R. Cormode, P. M. Lahti, *Org. Lett*., 2003, **5**, 2099.
67. G. M. Sheldrick, SHELXTL: Structure Determination Software Programs; Bruker Analytical X-ray Systems Inc.: Madison, WI, 1997.

